*Journal of the Korean Nuclear Society*
*Volume 13, Number 4, December, 1981*

**《Original》**

# Model Calculation of the Np-237 Fission Cross-Sections for $E_n = 0$ to 20 MeV

H.I. Bak*), B. Strohmaier and M.Uhl

Institut für Radiumforschung und Kernphysik der
Universität Wien, Austria
(Received August 1. 1981)

# 중성자 에너지 $E_n = 0$-20 MeV에 대한 Np-237 핵분열단면적의 모형계산

박혜일*), B. 스트로마이어 및 M. 울

오스트리아 비인대학교 라듐 및 핵물리연구소

(1981. 8. 1 접수)

**Abstract**

The Np-237 fission cross-sections up to 20 MeV incident neutron energy are calculated by means of the computer code STAPRE— a statistical model code with consideration of preequilibrium decay. The higher chance fissions up to third compound nucleus are taken into account, and the main input parameters in the treatment of fission under consideration of a double-humped fission barrier are carefully adjusted, so that the current trend of experimental data can be fitted within an apparent deviation of about 10% throughout the entire energy range. Results are presented in the form of point-wise cross-section values, and also in the form of graph to demonstrate the shape agreement.

**요 약**

예평형붕괴(預平衡崩壞)를 고려한 통계모형 전산코드 STAPRE를 써서 Np-237 핵분열 단면적을 입사중성자 에너지 20MeV까지 계산하였다. 중성자 방출에 수반되는 분열과정은 3차 복합핵까지 고려하였으며, 이중분열장벽(二重分裂障壁)에 관련된 주요 입력변수는 실험값의 최근 동향을 감안, 전 에너지 영역을 통하여 약 10%의 편차범위 내에서 부합될 수 있도록 조정하였다. 계산결과는 각 에너지에 대응하는 단면적 값의 표와, 실험값과의 비교를 제시하는 그림으로 나타냈다.

*) On leave from Department of Nuclear Engineering, Seoul National University, Seoul, Korea.

## I. Introduction

In the aspect of an increasing importance of accurate neutron nuclear data during the last decade, a great deal of effort has been devoted also to the refinement of fission cross-sections for a series of actinide nuclei. In particular, the theoretical scheme to estimate fission cross-sections based on elementary Hauser-Feshbach theory, developed in a coherent manner with the discovery of the double-humped fission barrier, has been realized as a powerful tool to provide a quantitative guidance for the cross-section evaluation. The object of this work has been to attempt such a model calculation to fit the experimental neutron induced Np-237 fission cross-sections in the energy range from threshold up to 20 MeV by use of the computer code STAPRE[1].

The Np-237 fission cross-section in the MeV energy range, due to the smooth excitation curve with incident neutron energy and the large cross-section values as well as the fission cross-section of U-238, has been considered as a promising neutron standard in neutron dosimetry connected with recent developments in fast reactor design, fast reactor safety and in fusion reactor technology, and the monoisotopic element of Np-237 is nowadays widely in use for application.

The trend of fission cross-section deduced from measurements has been fairly well established up to several MeV energy range[2,3]. However, it appears thus far that the status at the higher energy region is not quite apposite to the applications. For instance, a systematic discrepancy of about 20% or rather more with increasing energy above 9 MeV is observed between the earlier measurement of Pankratov (1963) and the recent measurement of Carlson and Patrik (1979), while the latter data are in good agreement in the entire energy region of interest with the cross-section values deduced from the accurate measurement of the cross section ratio with respect to U-235 fission cross-sections performed by Behrens et al. (1977), and thus these two sets of experimental data have been taken into account as a preferred measure of the present calculation for the higher energy range, in which the higher chance fission plays an essential role.

STAPRE is a statistical model code with consideration of preequilibrium decay for the emission of the first particle. The model assumptions employed in the code and the scheme of the parametrization for the input data will be quite briefly introduced in the following section (II). The input data for the fission cross section calculations are presented in section III, and at last the calculated results are compared with the existing experimental data (Section IV). The shape agreement seems reasonably good and the pointwise fitting with a discrepancy of 10% or less has been apparently realized due to the stepwise adjustment of the input parameters. To check the consistency of the model assumptions we additionally compared calculated $(n,\gamma)$ and $(n,2n)$ cross-sections with experimental data.

## II. Model Assumptions and Parametrizations

Detailed description of the STAPRE code with its original design philosophy, underlying physics and the practical features for applications has been presented by Uhl and Strohmaier[1]. From Ref. 1 the important concept of the model assumptions relevant for our problem will be briefly quoted in the following context with the input data preparation.

The code STAPRE is designed to calculate energy-averaged cross sections for particle-induced nuclear reactions including fission with several emitted particles (up to six) and gamma-rays under the assumption of sequential evaporation. Evaporation processes are treated within the framework of the statistical model with consideration of angular momentum and parity conservation. The equilibration of the composite system formed by incident particle and target nucleus is treated in the frame of the exciton model[4-7] which is considered as only one of the current models available for this process. In the preequilibrium stage of the reaction, particle emission is assumed to be the only decay mode; preequilibrium photon emission and fission are thus neglected.

A schematic diagram representing the proceeding of the code is given in Fig. 1 as a guide for understanding the application of these models and how the various models are combined with each other.

The term "$i^{th}$ compound nucleus (CN)" means the nucleus resulting from emission of ($i$-1) of a specified sequence of emitted particles ($\pi_1, \pi_2, \pi_3, \ldots$). Hence, the system formed by incoming particle $\pi_0$ and target nucleus $T$ is called first CN even if not yet in the equilibrium stage. Each CN is assumed to be subject to fission. Thus, higher chance fissions are treated as processes following the sequential particle evaporation steps.

The Hauser-Feshbach (HF) denominator $N(U,J,\Pi)$ is defined as the sum of transmission coefficients $T_c$ for all open channels $c$,

$$N(U,J,\Pi)=\sum_{c} T_c = N^{part}(U,J,\Pi) + N^{r}(U,J,\Pi) + N^{f}(U,J,\Pi) \quad (1)$$

and consists of contributions resulting from particle, gamma-ray and fission decay. The notation $U, J$ and $\Pi$ stands for the excitation energy, total angular momentum and parity, respectively. The program at first generates for each CN a table of the HF denominator $N_i(U,J,\Pi)$ and the fission probability $R_i^f(U,J,\Pi)$ corresponding to $i^{th}$ CN for all excitation energies $U$ (defined in steps by a grid of binsize DU) and all values of angular momentum $J$ and parity $\Pi$, which are required for the subsequent evaporation calculation. The symbol $WB_i^{(0)}(U,J,\Pi)$ represents the level population for $i^{th}$ CN resulting from the primary gamma-ray emission for $i=1$ and particle emission from the $(i-1)^{th}$ CN for $i\geq 2$, and $\overline{WB}_i(U,J,\Pi)$ gives the cumulative population due to the result of all possible gamma-ray cascades. For the equilibrium portion of first chance emission of particles and photons as well as for the first chance fission, the width fluctuation corrected HF formula is applied. For entrance channel $c$, exit channel $c'$, a total angular momentum $J$ and parity $\Pi$ the formula in well-known notation is given by

$$\sigma_{cc'}^{(HF)J\Pi}=\frac{\pi}{k^2}g^J\frac{T_cT_{c'}}{N_1(U,J,\Pi)}S_{cc'}^{J\Pi}, \quad (2)$$

where $S_{cc'}^{J\Pi}$ is the correction factor for the partial width fluctuation[8]. For the first chance fission cross-section one has to sum over all fission channels $c'$ and assign the important factor$_q^{pre}$ which is calculated in the framework of the exciton model and defnes ithefractional amount of the initial

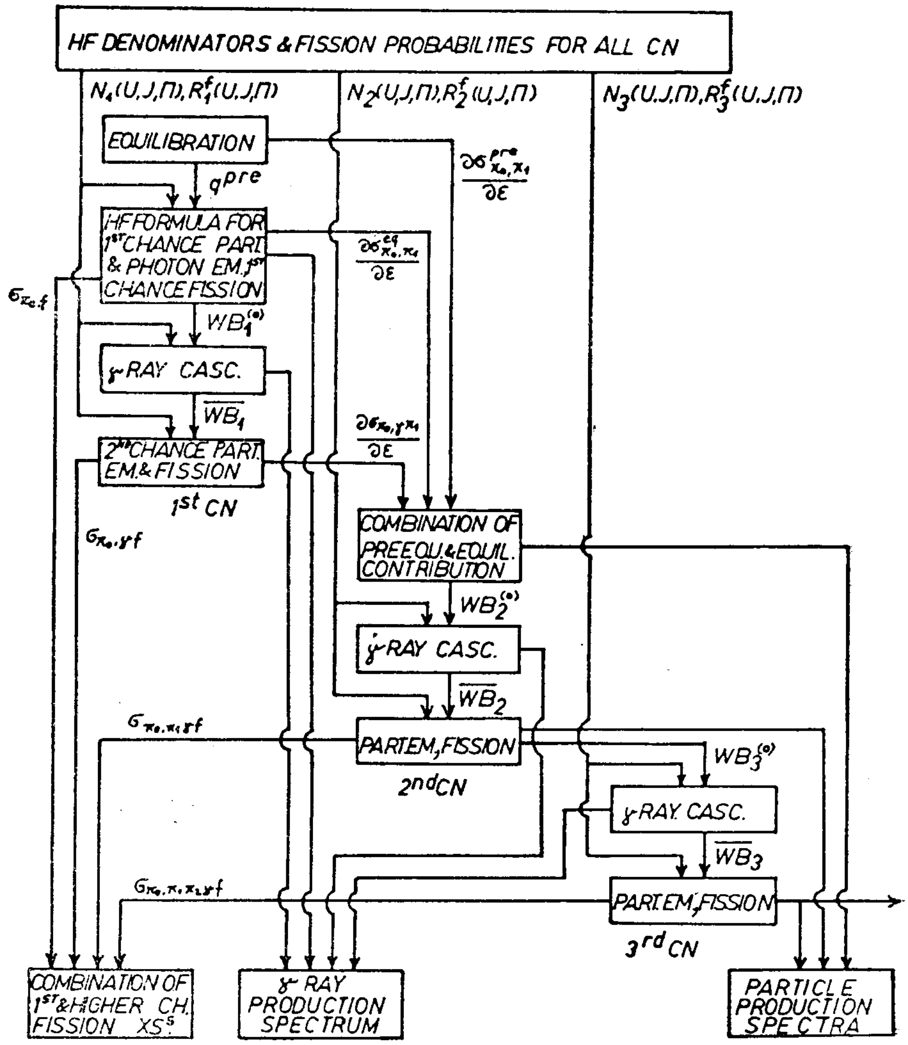


**Fig.1. A Schematic Representation of the Proceeding of the Code STAPRE.**

population surviving preequilibrium emission:

$$\sigma_{x_0,f}=q^{pre}\sum_{J'\Pi'}\sum_{cc'}\sigma^{(HF)J'\Pi'}_{cc'} \qquad (3)$$

The fraction $q^{pre}$ and the preequilibrium contribution to the differential cross-section with energy of relative motion (ε) are required for the further calculations as shown in Fig. 1. The higher chance contribution of the $i^{th}$ CN to the total fission cross-section is calculated from the fission probability $R_i^f(U,J,\Pi)$ and the cumulative population $\overline{WB}_i$ to take into account all processes with particle emission and gamma-ray cascades followed by fission;

$$\sigma_{x_0,x_1\cdots x_{i-1},f}=\sum_{J\Pi}\int_0^{U_{max}} dU\ \overline{WB}_i(U,J,\Pi)R_i^f(U,J,\Pi). \qquad (4)$$

Next, by referring to the original versions of STAPRE[9)10)] a certain extent of the fission model together with the parametrization of a double-humped fission barrier will be described.

i. Fission channels and fission cross-sections

The excited states of residual nuclei as well as the transition states at saddle-point deformation which both enter into the definition of the various channels are described by a level density $\rho(U,J,\Pi)$. At low excitation energy where the complete information to specify the discrete levels $(E_i, I_i, \Pi_i)$ is available the level density can be simply expressed as

$$\rho(U,J,\Pi)=\sum_j \delta(U-E_j)\,\delta_{JI_j}\delta_{\pi\pi_j}, \qquad (5)$$

while in the continuum the level density has to be calculated by means of a model.

The concept of fission transmission coefficients is based on the original statistical theory proposed by Bohr and Wheeler[11] together with the quantum-mechanical calculation of the tunnel penetrability for a parabolic barrier[12] characterized by the height $E$ and the curvature $\hbar\omega$. Then, the penetrability $P(U)$ is given by the well-known Hill-Wheeler formula;

$$P(U)=\frac{1}{1+\exp\left[\frac{2\pi}{\hbar\omega}(E-U)\right]} \qquad (6)$$

Under the assumption of a single-humped barrier one obtains for the transmission coefficient $T_c{}^f(U,J,\Pi)$ for fission decay of compound nucleus states with $(U,J,\Pi)$ via channel $c$

$$T_c{}^f(U,J,\Pi)=\delta_{J\Pi,\,I_c\pi_c}P_c(U)=\delta_{J\Pi,\,I_c\pi_c}\cdot\frac{1}{1+\exp\left[\frac{2\pi}{\hbar\omega}(E_c-U)\right]}, \qquad (7)$$

where $(E_c. I_c. \Pi_c)$ are the excitation energy, spin and parity of the transition state specifying the channel $c$. Hence, the fission contribution $N^f(U,J,\Pi)$ to the HF denominator becomes

$$N^f(U,J,\Pi)=\sum_c T_c{}^f(U,J,\Pi)=\int_0^\infty dE'\rho_f(E',J,\Pi)\cdot\frac{1}{1+\exp\left[\frac{2\pi}{\hbar\omega}(E_0+E'-U)\right]} \qquad (8)$$

where $\rho_f(E',J,\Pi)$ is the level density of the transition states and $E_0$ is the energy of the lowest transition state; $E'$ is the excitation energy of the transition states relative to $E_0$. The fission probability $R^f(U,J,\Pi)$ is the branching ratio for fission decay and thus given by

$$R^f(U,J,\Pi)=\frac{N^f(U,J,\Pi)}{N(U,J,\Pi)}. \qquad (9)$$

It has been indicated by recent studies that the actinide nuclei have so called double-humped fission barriers[13-18]. Therefore, this barrier shape and its consequences as intermediate class II structure and vibrational resonances should be taken into account in fission cross-section calculations.

The various $Np$ isotopes relevant to our problem are either odd or odd mass nuclei. The experimental $Np$-237 fission cross-section shows no clear structure due to vibrational resonances. Hence, we assumed complete damping of the fission mode in the secondary well. In the complete damping situation the inner barrier (barrier $A$) and the outer barrier (barrier $B$) act independently of each other[14]. When averaged with respect to intermediate class II structure the fission contribution to the HF denominator is given by

$$N^f(U,J,\Pi)=\frac{N_A{}^f(U,J,\Pi)N_B{}^f(U,J,\Pi)}{N_A{}^f(U,J,\Pi)+N_B{}^f(U,J,\Pi)}. \qquad (10)$$

In this expression, $N_A{}^f(U,J,\Pi)$ and $N_B{}^f(U,J,\Pi)$ are calculated according to eq. (8) for the inner and the outer barrier which are characterized by the heights $(E_A, E_B)$ and curvatures $(\hbar\omega_A, \hbar\omega_B)$ as shown

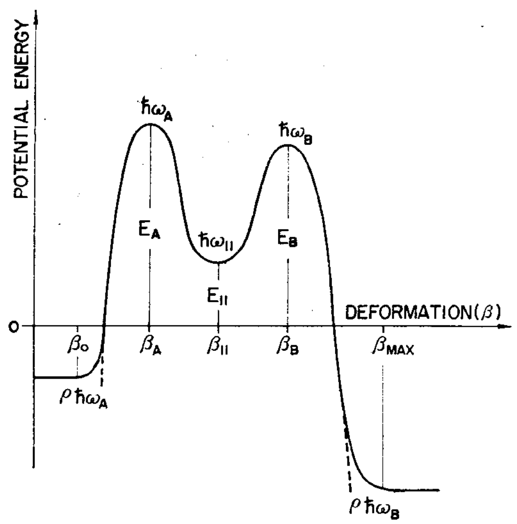


**Fig. 2. Schematic Diagram for Parametrization of Double-humped Fission Barrier.**

in the schematic diagram (Fig.2). As the specification of discrete transition states is important mainly for even nuclei, we described the complete spectrum for both barriers by a continuous level density formula(see section II. ii).

The fission probability $R^f(U,J,\Pi)$ entering in eq. (4) for the higher chance cross-sections has to be averaged over intermediate class II structure. This is done in the frame of the model of equidistant class II states with constant width proposed by Back et al.[14] One obtains in terms of the quantities $N^f(U,J,\Pi)$, defined in eq. (10), and $N'(U,J,\Pi)=N^{part}(U,J,\Pi)+N^r(U,J,\Pi)$:

$$R^f(U,J,\Pi)=\frac{N^f_{eff}(U,J,\Pi)}{N'(U,J,\Pi)+N^f_{eff}(U,J,\Pi)} \tag{11.1}$$

$$N^f_{eff}(U,J,\Pi)=$$

$$N^f\cdot\frac{1+\sqrt{1+\left(\frac{N'}{N^f}\right)^2+2\frac{N'}{N^f}\coth\left(\frac{N_A{}^f+N_B{}^f}{2}\right)}}{\frac{N'}{N^f}+2\coth\left(\frac{N_A{}^f+N_B{}^f}{2}\right)} \tag{11.2}$$

The effective fission contribution $N^f_{eff}$ $(U,J,\Pi)$ to the HF denominator is used as transmission coefficient of a group channel in the width fluctuation corrected HF formula (eqs. (2) and (3)). In this way the first chance cross-sections are approximately averaged with respect to intermediate class II structure.

ii. Level densities

Following the systematic study of Lynn[16] on the calculation of fission cross-sections of the actinide nuclei we used for the level densities at equilibrium and at the barrier deformations a combination of constant temperature and conventionally shifted Ferim-gas forms[19].

The following relation between the level density $\rho(U,J,\Pi)$ and the state density $\omega(U)$ holds:

$$\rho(U,J,\Pi)=\frac{1}{2}\rho(U,J)=\frac{1}{2}\frac{1}{\sqrt{8\pi}}\frac{1}{\sigma^3(U)}\cdot$$
$$\omega(U)(2J+1)\exp\left\{-\frac{\left(J+\frac{1}{2}\right)^2}{2\sigma^2(U)}\right\}. \tag{12}$$

Up to three regions with different energy dependence of the state density $\omega(U)$ and the spin cut-off parameter $\sigma(U)$ can be specified by the following forms:

$$O\leq U<U_1{}' : \omega(U)=C_1\exp\left\{\frac{U}{T_1}\right\},$$
$$\sigma(U)=\sigma_1 \tag{13.1}$$
$$U_1{}'\leq U<U_2{}' : \omega(U)=C_2\exp\left\{\frac{U}{T_2}\right\},$$
$$\sigma(U)=\sigma_2 \tag{13.2}$$
$$U_2{}'\leq U : \omega(U)=\frac{\sqrt{\pi}}{12}\cdot\frac{\exp[2\sqrt{a(U-\Delta)}]}{a^{1/4}\cdot(U-\Delta)^{5/4}},$$
$$\sigma^2(U)=\frac{1}{h^2}\Theta\,\mathrm{eff}\sqrt{\frac{U-\Delta}{a}} \tag{13.3}$$

The level parameters used in the model are the level density parameter a, the effective moment of inertia $\Theta$eff, the pairing correction $\Delta$, the constant factors $C_i$, the constant temperatnres $T_i$ and the spin cut-off parameters $\sigma_i$.

## Ⅲ. Summary of Input Data

The compound nuclei formed in sequence up to the fourth CN have to be specified in order to cover an energy range of 20 MeV. The control parameters concerned and the main input data considered as most essential to have influence upon the fitting calculation are itemized in the following:

i. Control parameters and energy binsize

In order to save computation time, the calculation of gamma-ray cascades can be suppressed for several CN. For the total number ($N$) of CN for a particular reaction the gamma-ray cascades can be optionally neglected for the CN with numbers $1, 2, \ldots, N_r < N$. In such cases the cumulative population $\overline{WB}_i$ is replaced by $WB_i^{(0)}$. At higher incident energies gamma-ray cascades for the first CN will be neglected by choosing $N_r = 1$.

As was shortly mentioned in section II, an energy grid with a binsized of $DU$ is introduced for the approximate integrations for the continuum region. The binsize $DU = 0.25$MeV has been assigned throughout the energy region from considerations of the numerical accuracy and the central memory as well as the computation time requirements. Since the HF denominator for each CN is stored binwise, the energy steps for the excitation function have to be chosen as integer multiples of $DU$. The energy step has been chosen as twice the binsize; i.e. 0.5MeV.

For the preequilibrium decay the parameter FM, which defines the magnitude of the matrix element for the internal transition rates, and the initial numbers of particles and holes have to be specified. The absolute square of the average effective matrix element of residual interactions is estimated in terms of the mass number A and the excitation energy $U$ by the following expression proposed by Kalbach-Cline[20]:

$$|M|^2 = FM \times A^{-3} U^{-1} \tag{14}$$

The value 263(MeV³) for FM has been selected from the test runs by using a range of values 220-320 together with the initial particle-hole numbers (2p, 1h). In addition, this value of FM reproduces at an excitation energy of 20MeV the internal transition rate for the (2p, 1h) configuration given by Gadioli et al.[21]

ii. Neutron optical potential

For the actinide region, a neutron-nucleus potential has been presented by Madland and Young[22]. This potential, however, is recommended only up to 20MeV. The real part of the potential as well as the imaginary part depends on energy rather strongly, and as for Np-237 there are no experimental data available at energies above 10MeV to verify the optical model parameters, this potential is not preferable for the present application.

Another potential has been derived by Lagrange[23] by means of optical model fits to the total neutron cross section and differential scattering cross-sections of $U$-238. This potential is recommended up to 20 MeV. We made use of this potential employing slight modifications described below.

The transmission coefficients for the statistical model input were generated by means of coupled channels calculations using a modified version of the Karlsruhe IUPITOR1 code[24,25]. The underlying physics are described in the earlier work of Tamura[26]. Real coupling was used. A Legendre expansion of the nonspherical potential was performed. We coupled only three states of the ground state rotational band: the $5/2^+$ ground state, the $7/2^+$ state at 33.2keV and the $9/2^+$ state at 75.8keV. For the calculations, coupling terms up to the order of $\lambda=8$ were included(for notation, see eq. (16) of Ref. 26). In the Legendre expansion of the potential a quadrupole and a hexadecupole deformation were taken into account, and characterized by the deformation parameters $\beta_2=0.240$ and $\beta_4=0.067$. These values differ from the deformation parameters given by Lagrange[23], for they were adjusted so as to reproduce the most recent experimental values[27] for the s-wave strength function for Np-237. Also, the constancy of the imaginary part for neutron energies above 10 MeV as prescribed by Lagrange[23] was changed into an increase like

$$6.7+0.1\times[E_n(\text{MeV})-10] \qquad (15)$$

in order to avoid a too strong decrease in the absorption cross-section above 10 MeV incident energy.

iii. Data required for the creation of gamma-ray transmission coefficients

Regarding gamma-decay the code is so designed that the maximum multipolarity of electric and magnetic radiation can be chosen less or equal three.

The gamma-ray transmission coefficient for transition energy $\varepsilon$ and multipole type XL is related to the gamma-ray strength function $f_{XL}^{\gamma}(\varepsilon)$

$$f_{XL}^{T}(\varepsilon)=2\pi\varepsilon^{2L+1}f_{XL}^{\gamma}(\varepsilon). \qquad (16)$$

For the $E1$ strength function the Brink-Axel model with global parameters for the giant $E1$ resonance[28] is used. The strength functions for $M1, E2, M2, E3$ and $M3$ radiation are chosen according to the Weisskopf model and normalized to $f_{E1}^{\gamma}$ by means of Weisskopf's estimate[29]. The final normalization of all gamma-ray transmission coefficients is carried out by fitting the average s-wave neutron radiation width $\bar{\Gamma}_\gamma$. The experimental values are compiled in the report BNL-325[30], and one can also refer to the more recent measurement of Mewissen et al.[27] and of Paya[31]. The experimental values of the s-wave neutron radiation width for Np-238 are scattered within the region roughly between 35 and 70 meV. The data required to be specified are the neutron separation energy $S_n$, spins of s-wave neutron resonances$(s_1, s_2)$ and the average total radiation width $\Gamma_\gamma$ at the neutron binding energy. The data used as the input for each CN are tabulated in Table 1.

**Table 1. Input Data Used for the Creation of Gamma-ray Transmission Coefficients.**

(*: **Ref. 16**)

| CN | $S_n$ (MeV) | $s_1^\pi$ | $s_2^\pi$ | $\bar{\Gamma}_\gamma$ (meV) |
|---|---|---|---|---|
| Np-238 | 5.486 | $2^+$ | $3^+$ | 38 |
| Np-237 | 6.591 | $11/2^-$ | $13/2^-$ | 62* |
| Np-236 | 5.691 | $2^+$ | $3^+$ | 60* |
| Np-235 | 6.992 | $1/2^+$ | | 65 |

iv. Barrier parameters and level densities

Input data for fission have to be arranged for all CN. As the symmetry properties of the saddle-point shapes are different at the two barriers, the spectrum of transition states has to be specified separately for the inner and the outer barrier.

According to the equations (2), (3), (4), (7), (8), (11.1) and (11.2) to calculate the fission cross sections, the barrier parameters($E_A, \hbar\omega_A, B_B, \hbar\omega_B$) as well as the level densities appear as the quantities having most influence on the result. In practice, the barrier parameters, especially the barrier heights, have been carefully adjusted within the frame of the systematics. As was expected from the Hill-Wheeler formula(eq. (6)), the adjustment of the curvatures presents a certain extent of fine control to fit the steepness of the excitation curve following on each threshold. The final sets of the barrier parameters are tabulated together with the values recommended by different authors in Table 2.

**Table 2. Barrier Parameters Used for the Present Calculation (top in each row), and Those Introduced by Different Authors.**

Unit: MeV

| CN | $E_A$ | $\hbar\omega_A$ | $E_B$ | $\hbar\omega_B$ | Ref. |
|---|---|---|---|---|---|
| Np-238 | 5.94 | 0.52 | 5.80 | 0.40 | |
| | 6.00±0.30 | 0.6 | 6.00±0.30 | 0.42 | (15) |
| | 6.19 | 0.65 | 5.99 | 0.45 | (16) |
| | 6.10 | 0.65 | 5.82 | 0.32 | (32) |
| Np-237 | 5.99 | 0.85 | 5.82 | 0.65 | |
| | 5.70±0.30 | 0.8 | 5.50±0.30 | 0.55 | (15) |
| | 5.9 | 0.8 | 5.6 | 0.5 | (16) |
| Np-236 | 6.05 | 0.60 | 6.03 | 0.40 | |
| | 5.70±0.30 | 0.6 | 5.2±0.30 | 0.42 | (15) |
| | 5.95 | 0.65 | 5.65 | 0.45 | (16) |
| Np-235 | 5.75 | 0.80 | 5.45 | 0.52 | |
| | 5.60±0.30 | 0.80 | 5.20±0.30 | 0.55 | (15) |
| | 5.75 | 0.80 | 5.45 | 0.52 | (16) |

As already mentioned in the foregoing section (II. ii), all transition states including the discrete part of the spectrum have been treated as continuum. The level density of transition states can be calculated by using the equations (12), (13.)-(13.3) in the same way as level densities for the continuum at equilibrium deformation. Level density parameters (see section II. ii) for the calculation of fission cross-sections for the actinide nuclei up to an incident energy of 3MeV have been recommended by Lynn[16-18]. For the level densities at equilibrium deformation in general we used Lynn's parameters. The only exception is Np-236 for which $C_1$ was decreased to one third of its original value in order to reduce the neutron emission probability from the second CN. As for the discrete part of the spectrum at equilibrium deformation, the data on the level scheme for each CN have been supplied from the Tables of Isotopes[33]. For the calculation of the barrier level densities, the values of the temperatures ($T_1, T_2$) and the spin-cutoff parameters($\sigma_1, \sigma_2$) are taken from the presentation of Lynn[16]. The parameters $C_1$ and $C_2$ have been adjusted together with the barrier heights to fit the experimental data possibly within an apparent deviation of about 10%. As Lynn's parameters for the transition state densities do not cover the energy range required for our calculations, we continuously joined a conventionally shifted Fermi gas formula at the upper end of the constant temperature region. The input level density parameters for the inner and the outer barriers of each CN are tabulated together with those for equilibrium deformation in Table 3. The pairing corrections ($\Delta$) for the CN with even neutron number are taken from the tabulation presented by Gilbert and Cameron[19]. The notation $\Theta$rig stands for the rigid body moment of inertia.

## IV. Results and Discussion

The final result of the Np-237 fission

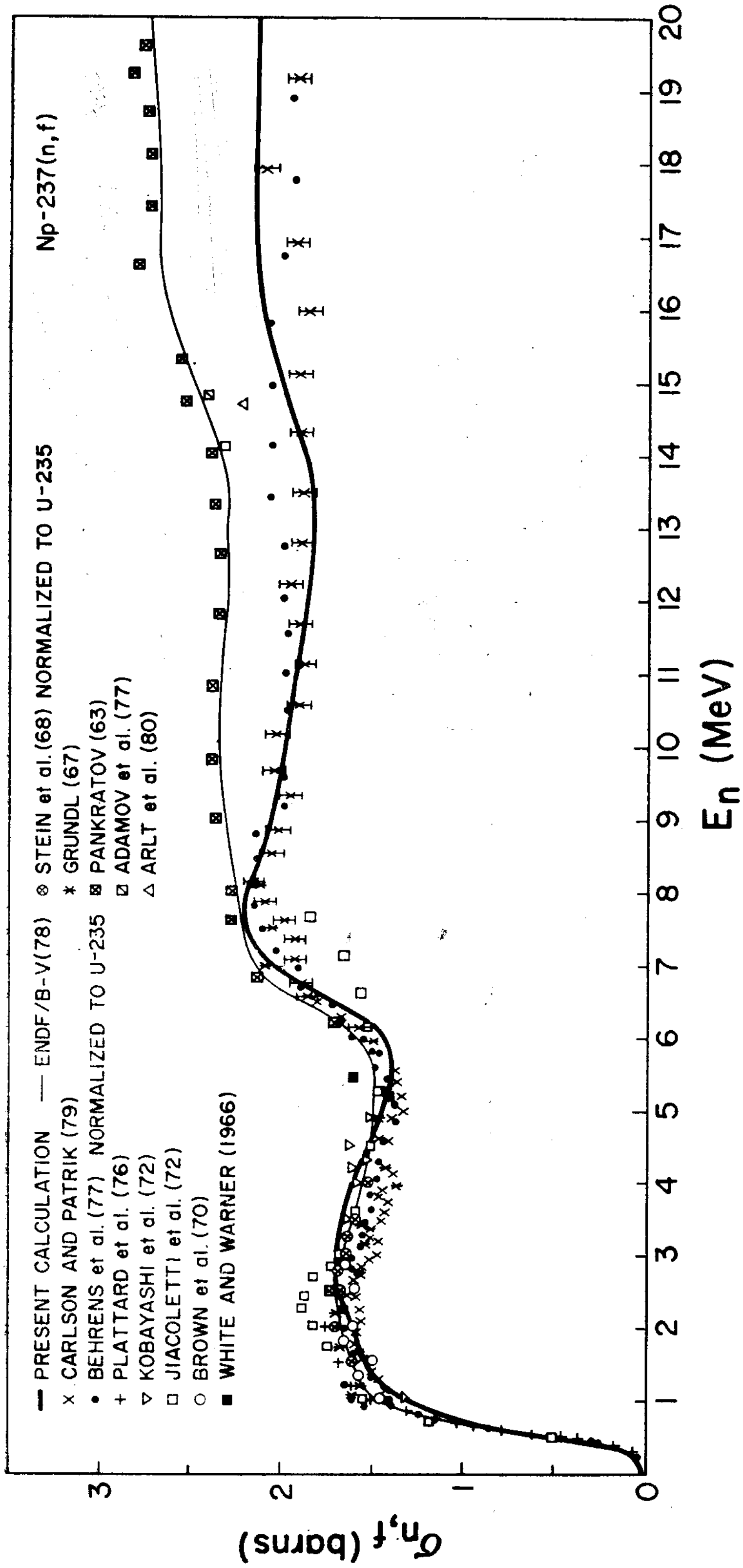


Fig. 3. Comparison of the Present Calculation of the Np-237 Fission Cross-section with Experiments.

**Table 3. Level Density Parameters for the Equilibrium and the Transition State Deformations. Values given at top for each compound nucleus correspond to the equilibrium deformation, and the next two rows are those for the barriers A and B, respectively.**

| CN | $a$ (MeV$^{-1}$) | $\theta$eff/ $\theta$rig | $\Delta$ (MeV) | $U_1'$ (MeV) | $C_1$ (MeV$^{-1}$) | $T_1$ (MeV) | $\sigma_1$ | $U_2'$ (MeV) | $C_2$ (MeV$^{-1}$) | $T_2$ (MeV) | $\sigma_2$ |
|---|---|---|---|---|---|---|---|---|---|---|---|
| | 28.00 | 0.842 | 0.00 | 2.92 | 4267. | 0.518 | 6.10 | | | | |
| Np-238 | 31.94 | 0.691 | 0.00 | 2.00 | 9068. | 0.360 | 6.40 | 6.00 | 42975. | 0.500 | 6.40 |
| | 30.33 | 0.673 | 0.00 | 2.00 | 4534. | 0.360 | 6.40 | 6.00 | 21488. | 0.500 | 6.40 |
| | 27.37 | 0.814 | 0.49 | 3.59 | 1203. | 0.500 | 6.10 | | | | |
| Np-237 | 30.06 | 0.925 | 0.49 | 3.69 | 2234. | 0.480 | 6.40 | | | | |
| | 27.92 | 0.891 | 0.49 | 3.69 | 1117. | 0.480 | 6.40 | | | | |
| | 26.51 | 0.973 | 0.00 | 2.15 | 1422. | 0.518 | 6.10 | | | | |
| Np-236 | 31.94 | 0.701 | 0.00 | 2.00 | 9068. | 0.360 | 6.40 | 6.00 | 42975. | 0.500 | 6.40 |
| | 30.33 | 0.683 | 0.00 | 2.00 | 4534. | 0.360 | 6.40 | 6.00 | 21488. | 0.500 | 6.40 |
| | 27.37 | 0.827 | 0.57 | 3.67 | 1024. | 0.500 | 6.10 | | | | |
| Np-235 | 32.33 | 0.940 | 0.57 | 4.00 | 4469. | 0.480 | 6.40 | | | | |
| | 30.18 | 0.908 | 0.57 | 4.00 | 2234. | 0.480 | 6.40 | | | | |

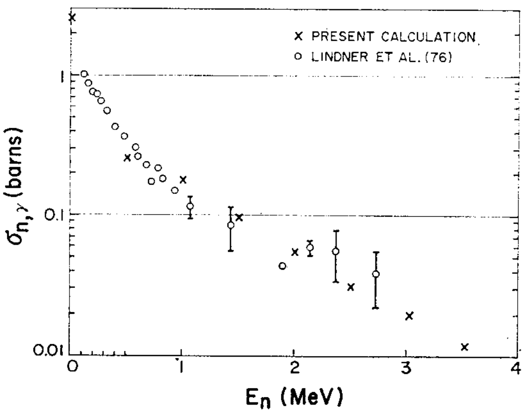


**Fig. 4. Comparison of the Calculated Np-237 Capture Cross-sections with Measurements.**

cross-section calculation is shown graphically in Fig.3 and also tabulated in Table 4. The recent data measured by different authors[34-45] are plotted in the same figure to demonstrate the overall features of the shape agreement. Each set of cross section ratios $\sigma_{n,f}$ (Np-237)/$\sigma_{n,f}$ ($U$-235) measured by Behrens et al.[39] and Stein et al.[41] are normalized by using the evaluated $U$-235 fission cross-sections of ENDF/B-V (78). For each data set measured by Plattard et a l.[38], Jiacoletti et al.[36] and Behrens et al.[39] only some of the numerous points are plotted in the first threshold region.

The calculated cross-section closely follows the experimental data in the threshold region up to~0.65MeV. Comparing with the main trend of the experimental data at the first plateau, the calculated value at 1MeV seems about 8% lower, while the values for3—4MeV stand somewhat higher, nevertheless the agreement with the measurements of Kobayashi et al., White and Warner, Stein et al. and Pankratov is fairly good. As an additional check of the model parameters in this energy range, the capturecross-sections calculated with the same input data are compared with the measurements of Lindner et al.[46] in Fig.4. The agreement seems quite reasonable.

For the higher energy region above~8 MeV, we attempted to reproduce the measurements of Carlson and Patrik[40]. These data were measured relative to the well determined hydrogen scattering cross-sect-

**Table 4. Calculated Fission Cross-sections from 0 to 20MeV.**

| Bombarding energy (MeV) | Fission cross section (barns) |
|---|---|
| 20. 06 | 2. 148 |
| 19. 54 | 2. 143 |
| 19. 03 | 2. 145 |
| 18. 51 | 2. 149 |
| 17. 99 | 2. 150 |
| 17. 48 | 2. 148 |
| 16. 96 | 2. 141 |
| 16. 44 | 2. 126 |
| 15. 93 | 2. 101 |
| 15. 41 | 2. 062 |
| 14. 89 | 2. 008 |
| 14. 38 | 1. 943 |
| 13. 86 | 1. 881 |
| 13. 34 | 1. 848 |
| 12. 83 | 1. 852 |
| 12. 31 | 1. 873 |
| 11. 79 | 1. 899 |
| 11. 28 | 1. 930 |
| 10. 76 | 1. 962 |
| 10. 24 | 1. 993 |
| 9. 728 | 2. 024 |
| 9. 211 | 2. 061 |
| 8. 695 | 2. 116 |
| 8. 178 | 2. 184 |
| 7. 662 | 2. 217 |
| 7. 145 | 2. 112 |
| 6. 629 | 1. 805 |
| 6. 112 | 1. 466 |
| 5. 596 | 1. 392 |
| 5. 079 | 1. 451 |
| 4. 563 | 1. 528 |
| 4. 046 | 1. 637 |
| 3. 529 | 1. 669 |
| 3. 027 | 1. 705 |
| 2. 525 | 1. 690 |
| 2. 022 | 1. 603 |
| 1. 520 | 1. 555 |
| 1. 018 | 1. 277 |
| 0. 516 | 0. 637 |
| 0. 014 | 0. 020 |

ions with an annular proton telescope and extend from 1-20MeV with and error limit of 2—3% throughout the energy region.

The data are plotted in Fig. 3 as read off the graphic representation (Fig.10 of Ref. 40) and found to be in good agreement with the cross-section values deduced from the precise fission ratio measurements of Behrens et al.[39]. The results fitted to the above data sets seems still in agreement with Pankratov's data up to 8MeV. The calculations show a more pronounced third plateau than the data of Carlson and Patrik[40] and of Behrens et al.[39] do although the barrier heights for the third CN have been remarkably increased to suppress the third chance fission. On the other hand, it has been inevitable to meet with a certain increase of the competitive cross-section $\sigma_{n,xn}$. The calculated cross-sections for the reaction Np-237$(n, 2n)$ Np-236 are compared with the existing experimental data[47-50] in Fig.5. The calculation exceeds

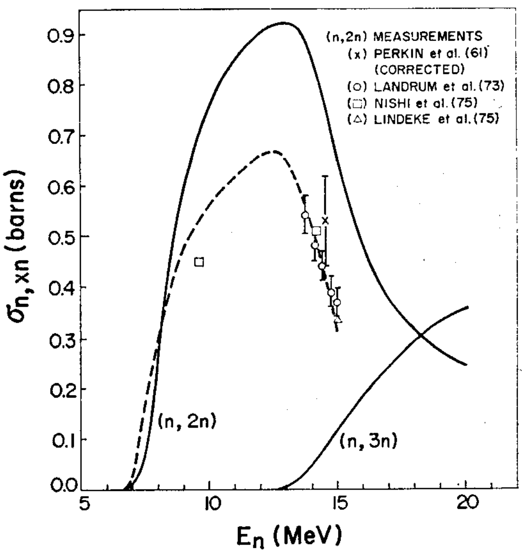


**Fig. 5. Calculated Np-237 (n, xn) Cross-sections. ----Caner et al. (77) (Ref. 54)**

by at least 0. 4 barns the quoted measurements or the evaluation of Caner et al.[51] in the 14 MeV region. Most of the $(n, 2n)$ measurements reter to the 22. 5$h$ activity but not to the long-lived activity ($1.3\times10^6$ *a*). The deduced total (*n*, 2*n*) cross-sections rely on the production cross-section ratio of long-lived to short-lived activity. Only one measurement of the production of the long-ived activity has been performed using the intense thermonuclear neutron flux of a nuclear device as described in Ref 48. Therefore the quoted measurements hardly provide a base to disprove the calculation. Of course, there remains the question whose measurements of the fission cross-section at higher energies are more reliable. A calculation which reproduces Pankratov's fission cross-section would result in (*n*, 2*n*) cross-sections in much better agreement with the data of Refs. 47-50. As a most recent 14MeV fission cross-section, the absolute measurement of Arlt et al.[44] presented the value of ($2.226\pm0.024$) barns at 14.70 MeV which lies nearly at the middle between the data of Pankratov and those of Carlson et al.


### Acknowledgements

The authors wish to thank Prof. H. Vonach for the kind encouragement, and the IAEA Nuclear Data Section for providing the useful cross-section data in the format of EXFOR and other important references.

One of the authors (H.I. Bak) would like to use this opportunity to express his thanks to Prof. P. Weinzierl for the warm hospitalities extended to him at the Institut für Experimentalphysik, and to acknowledge with thanks the financial support provided by the Ministry of Education, Republic of Korea, in form of a research grant.


### References


1) B. Strohmaier, M. Uhl, "Nuclear Theory for Applications", International Centre for Theoretical Physics, Trieste, 1978, p.313-326 (1980).
2) S. Cierjacks, *Symp. on Neutron Standards and Applications*, National Bureau of Standards, Gaithersburg, 77 NBS 278(1977).
3) H.I. Bak and A. Lorenz, *J. of Kor. Nucl. Soc.*, **3**, 77(1971).
4) J.J. Gritfin, *Phys. Lett.*, **17**, 478(1966).
5) C.K. Cline and M. Blann, *Nucl. Phys.*, **A172**, 225(1971).
6) E. Gadioli, E. Gadioli-Erba and P.G. Sona, *Nucl. Phys.*, **A217**, 589(1973).
7) C. Kalbach, *Acta Phys. Slovaca*, **25**, 100(1975).
8) P.A. Moldauer, *Revs. of Mod. Phys.*, **36**, 1079 (1964).
9) M. Uhl and B. Strohmaier, "STAPRE-A Computer Code for Particle Induced Activation Cross Sections and Related Quantities", IRK 76/01, University of Vienna(1976), unpublished
10) M. Uhl and B. Strohmaier, "Addenda to IRK 76/01, Jan. 1978", University of Vienna(1978), unpublisned
11) N. Bohr and J.A. Wheeler, *Phys. Rev.*, **56**, 246 (1939).
12) D.L. Hill and J.A. Wheeler, *Phys. Rev.*, **89**, 1102(1953).
13) M. Brack, J. Damgaara, A.S. Jensen, H.C. Pauli, V.M. Strutinsky, C.Y. Wong, *Revs. of Mod. Phys.*, **44**, 320(1972).
14) B.B. Back, O. Hansen, H.C. Britt and J.D. Garrett, *Phys. Rev.*, **C9**, 1924(1974).
15) B.B. Back. H.C. Britt, O. Hansen and B. Leroux, *Phys. Rev.*, **C10**, 1948(1974).
16) J.E. Lynn, Rept. AERE Harwell R 7468(1974).
17) A. Michaudon, "Neutrons and Fission", *Int. Conf. on the Interaction of Neutrons with Nuclei*, Lowell, Mass., July 1976
18) J.E. Lynn, "Nuclear Theory for Applications", International Centre for Theoretical Physics, Trieste, 1978, p.353-415(1980).
19) A. Gilbert and A.G.W. Cameron, *Can. J. Phys.*, **43**, 1446(1965).
20) C. Kalbach-Cline, *Nucl. Phys.*, **A210**, 590 (1973).

21) E. Gadioli, E. Gasioli-Erba and J.J. Hogan, *Phys. Rev.*, **C16**, 1404(1877).
22) D.G. Madland and P.G. Young, *Proc. Int. Conf. on Neutron Physics and Nucl. Data for Reactors and other Applied Purposes*, Harwell, U.K., 1978, p.349(1978).
23) C. Lagrange, *Acta Phys. Slovaca*, **26**, 32(1976).
24) T. Tamura, Rept. ORNL-4152(1967).
25) H. Rebel and G.W. Schweimer, Rept. KFK-1333(1971).
26) T. Tamura, *Revs. of Mod. Phys.*, **37**, 679(1965).
27) L. Mewissen et al., *Nucl. Sci. Eng.*, **70**, 155 (1979).
28) P. Axel, *Phys. Rev.*, **126**, 671(1962).
29) V.F. Weisskopf, *Phys. Rev.*, **83**, 1073(1951).
30) S.F. Mughabghab and D.J. Garber, BNL-325, 3rd(1973).
31) D. Paya, FRNC-TH-341(1972).
32) M. Di Toro and G. Russo, *Nucl. Phys.*, **284**, 177(1977).
33) C.M. Lederer and V.S. Shirley, "Table of Isotopes" (Seventh Ed.), John Wiley and Sons, Inc.(1978).
34) P.H. White, Rept. EANDC(UK)-77 (1966); EXFOR 21195(1980).
35) W.K. Brown, D.R. Dixon and D.M. Drake, *Nucl. Phys.*, **A156**, 609(1970).
36) R.J. Jiacoletti, W.K. Brown and H.G. Olson, *Nucl. Sci. Eng.*, **48**, 412(1972).
37) K· Kobayashi, I. Kimura, H. Gotoh and H. Yagi, EANDC(J)-26, 39(1972); EXFOR 20300 (1974).
38) S. Plattard, J. Blons, D. Paya, *Nucl. Sci. Eng.*, **61**, 477(1976).
39) J.W. Behrens, J.W. Magana and J.C. Browne, Rept. UCID-17370(1977).
40) A.D. Carlson and B.H. Patrik, *Proc. Int. Conf. on Nucl. Cross Sections for Technology*, Knoxville, Tennessee, 1979, IB4(1979).
41) W.E. Stein, R.K. Smith and H.L. Smith, Rept. LA-DC-9205(1968).
42) J.A. Grundl, *Nucl. Sci. Eng.*, **30**, 39(1967).
43) V.M. Pankratov, *Atomnaja Energija*, **14**, 177 (1963); EXFOR 80061(1972).
44) R. Arlt et al., Conf. Rept. ZFK-410(1980); EXFOR 30475(1981).
45) V.M. Adamov et al., *Symp. on Neutron Standards and Applications*, National Bureau of Standards, Gaithersburg, 77NBS 313(1977).
46) M. Lindner, R.J. Nagle and J.H. Landrum, *Nucl. Sci. Eng.*, **59**, 381(1976); EXFOR 10221 (1976).
47) J.L. Perkin and R.F. Coleman, *J. Nucl. Energy*, **14**, 69(1961).
48) J.H. Landrum, R J. Nagle and M. Lindner, *Phys. Rev.*, **C8**, 1938(1973).
49) T. Nishi, I. Fujiwara and N. Imanishi, NEA-NDC(J)-42L (1975); EXFOR 20692(1976).
50) K. Lindeke, S. Specht and J. Born, *Phys. Rev.*, **C12**, 1507(1975).
51) M. Caner, S. Wechsler and S. Yiftah, Rept. IA-1346(1977).